

Cite this: *Org. Biomol. Chem.*, 2023, **21**, 1549

Generating water/MeOH-soluble and luminescent polymers by grafting 2,6-bis(1,2,3-triazol-4-yl)pyridine (btp) ligands onto a poly(ethylene-*alt*-maleic anhydride) polymer and cross-linking with terbium(III)[†]

Isabel N. Hegarty,^a Adam F. Henwood,^{a,b} Samuel J. Bradberry^{*a} and Thorfinnur Gunnlaugsson ^{*a,b}

The synthesis of two new polymers made from **P(E-*alt*-MA)** (poly(ethylene-*alt*-maleic anhydride) and possessing 2,6-bis(1,2,3-triazol-4-yl)pyridine (**btp**) ligand side chains in 3 and 6 mol%, respectively (**P1** and **P2**, respectively) is described. These polymers were shown to be soluble in MeOH solution and, in the case of **P1**, also in water, while **P2** needed prolonged heating to enable water dissolution. **Btp** ligands are known for coordinating both d- and f-metal ions and so, herein, we demonstrate by using both UV-Vis absorption, fluorescence emission, as well as time-gated phosphorescence spectroscopies, that both **P1** and **P2** can bind to Tb(III) ions to give rise to luminescent polymers. From the analysis of the titration data, which demonstrated large changes in the emission intensity properties of the polymer upon Tb(III) binding (ground state changes were also clearly observed, with the absorption being red-shifted at lower energy), we show that the dominant stoichiometry in solution is 1 : 2 (M : L; Tb(III) : **btp** ratio) which implies that two **btp** ligands from the polymer background are able to crosslink through lanthanide coordination and that the backbone of the polymer is very likely to aid in coordinating the ions.

Received 14th December 2022,
Accepted 24th January 2023

DOI: 10.1039/d2ob02259a

rsc.li/obc

Introduction

The development of functional and robust materials with unique properties is highly topical within the areas of supramolecular and materials chemistries.^{1–3} As part of such developments the formation and study of responsive luminescent and/or supramolecular polymers is gaining significant interest.^{4–6} For over a decade now we have been reporting examples of both all-organic and lanthanide-based polymers and soft-materials (such as self-assembled gels and cross-linked supramolecular polymers) formed by using lanthanide coordinating ligands such as cyclens (1,4,7,10-tetraazacyclododecanes) and self-recognising, hydrogen bond-driven self-assembling BTAs (benzene-1,3,5-tricarboxamides).^{7,8} In particular, we have been interested in probing the evolution of the

photophysics of such systems upon coordination to various lanthanide ions,⁹ especially as many lanthanides possess unique and desirable luminescence properties such as long-lived excited states and emissions occurring at long wavelengths with line-like features.¹⁰ Such properties have applications in various fields including optoelectronics,¹¹ medicine,¹² chemosensing,¹³ counterfeiting,¹⁴ *etc.* Furthermore, depending on the coordination properties of the ligands employed, they can also be used as cross-linking agents within supramolecular polymers, rendering such polymers with additional properties.¹⁵

The 2,6-bis(1,2,3-triazol-4-yl)pyridine (**btp**) structure is an attractive ligand that has been used in various areas of research.¹⁶ In particular, the **btp** has been employed in coordination chemistry, due to its similarity to the well-known **terpy** ligand.¹⁷ Recently, Byrne *et al.* utilised this ligand upon complexation to Ru(II) in antifouling¹⁸ as well as in the formation of chiral luminescent lanthanide complexes that give rise to circularly polarised luminescence (CPL) from the lanthanide centre.¹⁹ In addition to its favourable metal ion coordination properties, the **btp** motif has been shown to form dimers *via* self-templation. This was recently demonstrated by our research group where we exploited the self-templating features

^aSchool of Chemistry and Trinity Biomedical Sciences Institute (TBSI), Trinity College Dublin, The University of Dublin, Dublin 2, Ireland. E-mail: gunnlaut@tcd.ie, bradberry.samuel@gmail.com

^bSynthesis and Solid-State Pharmaceutical Centre (SSPC), School of Chemistry, Trinity College Dublin, The University of Dublin, Dublin 2, Ireland

[†]Electronic supplementary information (ESI) available: Characterisation and NMR studies. See DOI: <https://doi.org/10.1039/d2ob02259a>



of both chiral as well as achiral olefin **btp** precursors to synthesise homocircuit [2]catenanes and pseudo-rotaxanes using ring closing metathesis (RCM) reactions.^{20,21} We have also been interested in the use of **btp** complexes in the formation of responsive polymers, and demonstrated that such complexes can be incorporated into HEMA polymers.²² However, since these complexes are doped non-covalently into the polymer hosts, they are prone to leaching from the material during solvent swelling processes. With this in mind, we recently developed **btp** monomers possessing a methacrylamide unit which could be co-polymerised with 2-hydroxyethyl methacrylate (HEMA), methylmethacrylate (MMA) and ethylene glycol dimethacrylate (EGDMA) to give polymers containing covalently attached **btp** units.²³ This gave rise to a hard 'plastic' like material that was luminescent upon treatment with lanthanide ions such as Eu(III) and Tb(III). While being highly successful, unfortunately this method sometimes resulted in the formation of films that lacked homogeneity upon treatment with the lanthanides. With this in mind, we set out to develop poly(ethylene-*alt*-maleic anhydride) [P(E-*alt*-MA)]^{24,25} polymers as the basis for new, alternative, **btp**-containing polymers that were soluble in competitive media and would give more consistent homogeneity within their structures upon doping with lanthanides.

Results and discussion

Design, synthesis and NMR characterisations of P1 and P2

The P(E-*alt*-MA) polymer is water soluble in moderate alkaline environments as, upon polymerisation, each anhydride moiety is converted into two carboxylate groups.²⁶ An important application of this polymer is in rendering water-soluble compounds insoluble for extraction from aqueous environments.²⁷ The anhydride functionality of this polymer has been shown to react readily with even moderate nucleophiles, undergoing a variety of reactions including amidation, esterification, hydrolysis, thioesterification, and imidization, generating a functionalised water-insoluble polymer.^{28,29} In our previous work within this area of research, we developed the **btp** ligand **1** as an intermediate in the formation of the methacryloyl amide based **btp** ligands.²³ This final structure was then incorporated by co-polymerisation into a hydrogel polymer using HEMA, MMA and EGDMA.²³ Here, however, we generated the polymers **P1** and **P2** in a single step, with a low loading of compound **1**, from P(E-*alt*-MA), Fig. 1.

The synthesis of **P1** was achieved by first dissolving P(E-*alt*-MA) in anhydrous DMF and, to this solution, 3 mol% of ligand **1** in DMF was added dropwise. The reaction was complete after one hour, and the **P1** polymer was isolated by dropping the reaction mixture into 0.5 M HCl. This caused the formation of a white precipitate, which was isolated by filtration, followed by washing with water to yield the pure product. This procedure was repeated using 6 mol% of ligand **1** to generate polymer **P2**. The resulting polymers were characterised by NMR spectroscopies. The ¹H NMR of **P1** is shown in Fig. 2,

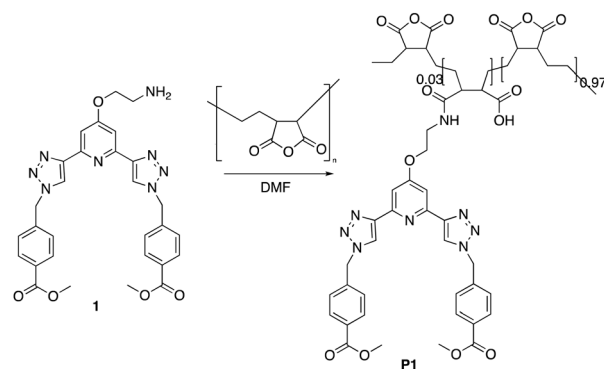


Fig. 1 The polymer **P1** formed by grafting the **btp** ligand **1** onto poly(ethylene-*alt*-maleic anhydride) [P(E-*alt*-MA)] (**P2** was formed in a similar manner).

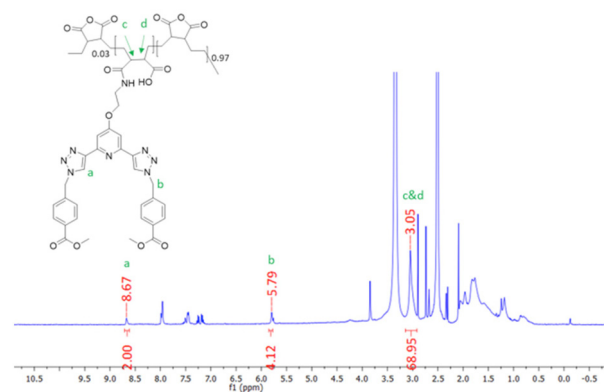


Fig. 2 The ¹H NMR spectrum (600 MHz, DMSO-*d*₆) of **P1**.

while the ¹³C NMR of **1** (top) and **P1** (bottom) are shown in Fig. 3.

As demonstrated in Fig. 2, ¹H NMR (600 MHz, DMSO-*d*₆) studies were used to confirm the formation of the grafted polymer **P1**. The resonance corresponding to the triazole protons occurs at 8.67 ppm, which is at a similar resonance to the analogous proton in the free ligand **1**. The signal at 5.79 ppm can be assigned to the CH₂ protons of ligand **1**. The signal upfield at 3.05 ppm corresponds to protons *c* and *d* of the polymer backbone, while the remaining protons of the polymer chain resonate as a broad signal at approximately 0.85–1.96 ppm. Integration of the ¹H NMR peaks confirmed an approximately 3% loading of compound **1** onto the polymer backbone.

As shown in Fig. 3, ¹³C NMR spectroscopy also confirmed the formation of the desired product **P1**. The appearance of two signals at 175.1 and 173.6 ppm in the polymer ¹³C NMR are indicative of the carbonyl carbons of the polymer backbone while the carbonyl carbon associated with the arms of ligand **1** is located at 165.9 ppm. Additional resonances are also visible in the base line, that are more deshielded within the polymer structure. The formation of **P2** was also confirmed by NMR spectroscopies (see ESI†).



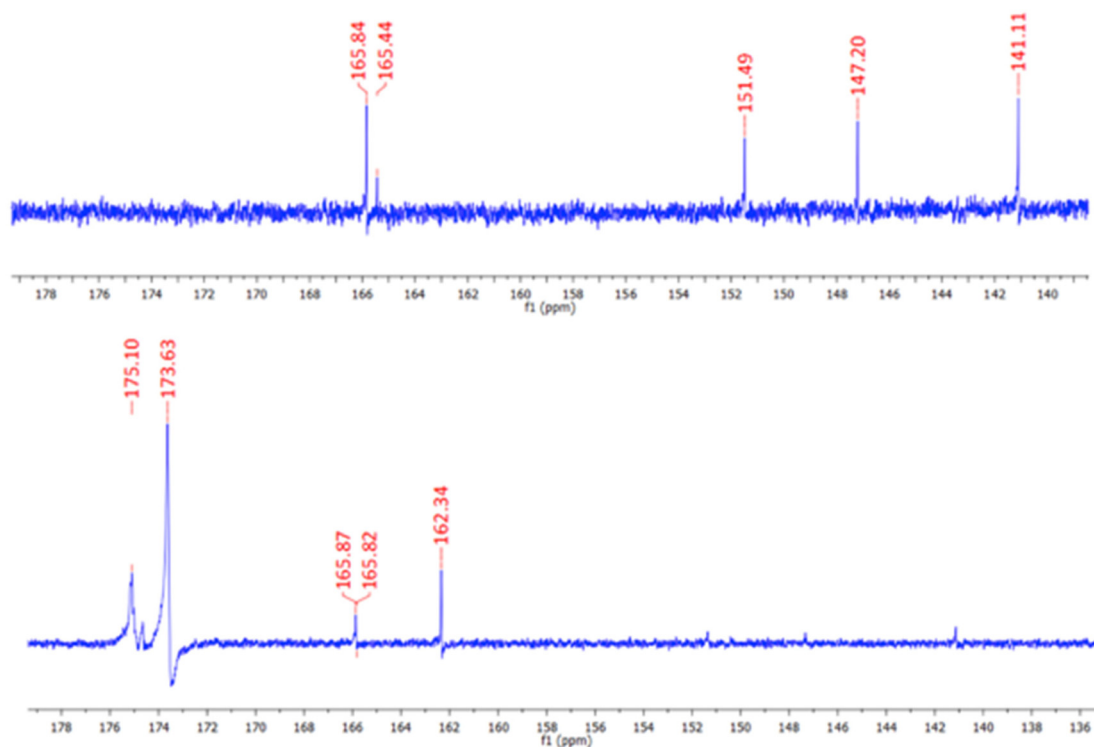


Fig. 3 The ^{13}C NMR spectra (600 MHz, $\text{DMSO}-d_6$) of **1** (top) and **P1** (bottom). The resonances assigned to the ligand are also clearly visible.

Solution studies of **P1** and **P2**

As mentioned above, the objective herein was to develop simple, water-soluble, lanthanide-based polymers. Although **P2**, which was soluble in CH_3OH , could only dissolve in water after prolonged heating at $60\text{ }^\circ\text{C}$ for several days, it was gratifying to find that, upon solvation, polymer **P1** was found to readily dissolve in both CH_3OH and water (*cf.* as demonstrated with a picture shown as insert in Fig. 4). Addition of the polymers to water gave a colourless solution in the case of **P1** and a more viscous, and white suspension in the case of **P2**. By contrast, both polymers readily dissolved in CH_3OH , generated a colourless solutions (see inset in Fig. S2 ESI †).

The UV-visible absorption and fluorescence emission spectra of **P1** and **P2** were recorded in both H_2O and CH_3OH and are shown in Fig. 4. In all cases there were two main

bands observed in the UV-visible absorption spectra at $\lambda_{\text{max}} = 231\text{ nm}$ and $\lambda = 298\text{ nm}$. As would be expected, the features of the absorption spectra of both polymers resemble that of the **btp** ligands with only a slight loss of resolution in the band at 298 nm , confirming that the **P(E-alt-MA)** polymer does not significantly interfere with the absorption profile of compound **1**. This provides a useful spectroscopic handle for monitoring the evolution of the self-assembly of our polymers by UV-visible absorption spectroscopy (*vide infra*). Upon excitation of the **btp** within the polymers ($\lambda_{\text{exc}} = 240\text{ nm}$) ligand-centred fluorescence was observed ($\lambda_{\text{max}} = 323\text{ nm}$) which is characteristic of the photophysical behaviour of many **btp** ligands.³⁰

Solution studies of **P1** and **P2** in the presence of Tb(III)

In our previous works we have demonstrated the efficacy of **btp** ligands in binding lanthanide ions and giving rise to highly luminescent complexes.³¹ This is particularly the case with Tb(III) ions whose resultant complexes exhibit photoluminescent quantum yields that are almost an order of magnitude higher than those measured for analogous Eu(III) complexes in organic solutions. This has been ascribed to well-matched energy levels between the triplet state of the **btp** and Tb(III) . Thus, with this in mind, we next investigated the use of Tb(III) ions for cross-linking polymer chains of **P1** and **P2**: by titrating CH_3OH solutions of these polymers with Tb(III) , we could monitor changes in both the ground and the excited states of these polymers as they undergo cross-linking. CH_3OH was chosen to minimise any quenching of the Tb(III) excited state

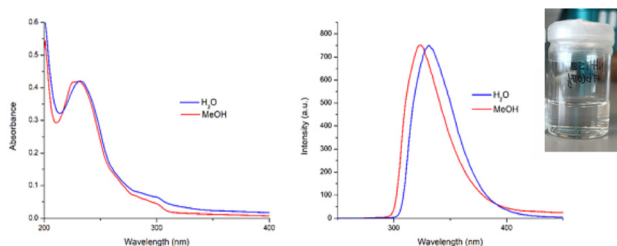


Fig. 4 (Left) Overlaid absorption spectra of **P1** in H_2O and CH_3OH and (right) fluorescence spectra of **P1** in H_2O and CH_3OH recorded at a concentration of approximately $c \sim 6 \times 10^{-6}\text{ M}$. Inset: A photograph of **P1** dissolved in H_2O demonstrating the transparent nature of the solution.



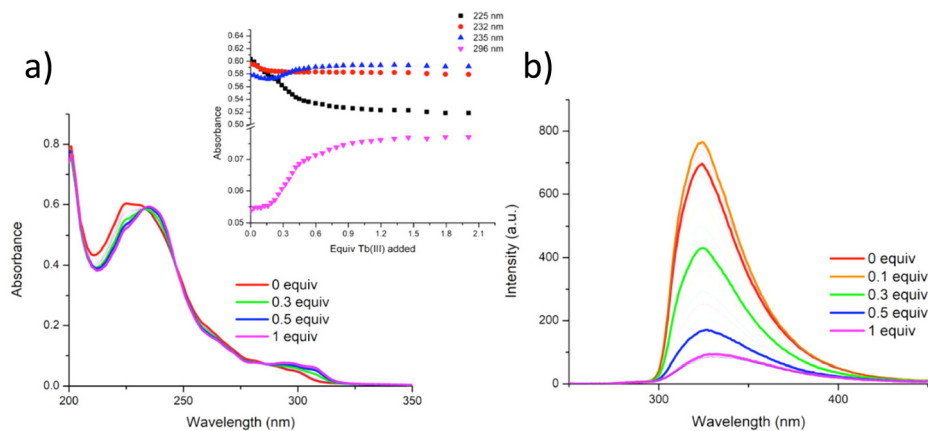


Fig. 5 (a) The overall changes in the UV-vis absorption spectra, and (b) fluorescence spectra ($\lambda_{\text{exc}} = 237$ nm) upon titrating **P1** (1×10^{-5} M within **P1**) against $\text{Tb}(\text{CF}_3\text{SO}_3)_3$ (0 \rightarrow 3 equiv.) in CH_3OH at RT. Inset (a): corresponding experimental binding isotherms of absorbance at $\lambda = 325, 232, 235$ and 295 nm.

from water oscillators. The solutions of **P1** and **P2** were prepared so that the overall concentrations of the **btp** units within the solutions were 1×10^{-5} M. These solutions were then titrated against specific aliquots of $\text{Tb}(\text{CF}_3\text{SO}_3)_3$, and the changes to the UV-visible absorption, ligand fluorescence, and delayed lanthanide luminescence were analysed.

Ground state changes. As can be seen from Fig. 5a, for **P1**, the two main absorptions bands centred at 227 nm and 298 nm were affected by the addition of $\text{Tb}(\text{CF}_3\text{SO}_3)_3$ to the solution, which is indicative of complex formation between the **btp** ligands and $\text{Tb}(\text{III})$. The band centred at 227 nm underwent a hypochromic and concomitant redshift up to the addition of 0.3 equivalents of $\text{Tb}(\text{III})$. From 0.3 \rightarrow 0.5 equivalents of $\text{Tb}(\text{III})$ solution a further increase in the absorbance was observed and the band was shifted to 236 nm, after which the changes reached a plateau. The band located at 298 nm experienced a hyperchromic shift and was accompanied by the formation of a new maximum at 306 nm. These changes occurred up to the addition of 1 equivalent of $\text{Tb}(\text{III})$. Three isosbestic points at 232 nm, 247 nm and 286 nm were also observed, pointing toward the presence of two distinct species in solution. This would indicate that two **btp** units are associating within the polymer for each $\text{Tb}(\text{III})$ ion, and that cross-linking between polymers would be occurring within the polymer matrix.

In a similar manner the changes in the absorption spectra of **P2** upon addition of $\text{Tb}(\text{CF}_3\text{SO}_3)_3$ were also monitored. As for **P1**, the absorption spectrum of **P2** consisted of two main bands located at 231 nm and 296 nm, respectively (see ESI[†]), and three isosbestic points were observed at 233 nm, 246 nm and 287 nm, respectively. Upon addition of $\text{Tb}(\text{III})$, the higher energy band experienced a redshift and concomitant decrease in absorbance up to the addition of 0.5 equivalents of $\text{Tb}(\text{III})$. Subsequently, this band increased upon addition of further 0.5 equivalents of $\text{Tb}(\text{III})$. There were also changes at longer energy with the band centred at 296 nm experiencing a hyperchromic shift (see ESI[†]). These changes also occur up to the

addition of 0.5 equivalents of $\text{Tb}(\text{III})$. From the changes to the UV-visible absorption and luminescence spectra, it can be concluded that multiple species coexist in solution. As the most significant changes to the spectra occur up to the addition of 0.5 equivalents of $\text{Tb}(\text{III})$, it is likely that the more emissive $\text{M}:\text{L}_3$ and/or $\text{M}:\text{L}_2$ species are the ones generated. The speciation above 0.5 equivalents does not appear to undergo changes upon the addition of excess $\text{Tb}(\text{III})$, and thus suggests there is unlikely to be any dissociation to the less emissive ML species.†

Singlet excited state (fluorescence) changes. Having examined the changes in the ground state, we next investigated the changes in the ligand centred emission as a function of $\text{Tb}(\text{III})$ content. Upon excitation of **P1** at 237 nm, **btp**-based, ligand centred emission was observed at 332 nm (Fig. 5b). However, upon titrating **P1** with a solution of $\text{Tb}(\text{CF}_3\text{SO}_3)_3$, the **btp**-based fluorescence underwent significant fluorescence quenching as the polymer ligand was coordinated by the metal ion. Up to the addition of 0.5 equivalents of $\text{Tb}(\text{III})$, a 79% reduction in the ligand-based emission was observed. This reduction continued until 1.0 equivalents of $\text{Tb}(\text{III})$, upon which the emission plateaued at 10% of the initial ligand-centred emission. This quenching is attributed to an efficient energy transfer process from the **btp** unit within the polymer to the ⁵D₄ $\text{Tb}(\text{III})$ -centred excited state, which itself precedes relaxation to the ground state *via* characteristic $\text{Tb}(\text{III})$ -based, green emission (*vide infra*).³² This efficient quenching also points toward the formation of a cross-linked polymer where different **btp** moieties of neighbouring polymer chains indivi-

† The fitting of the changes in the acetamide version of **1** (to prevent PET from the free amine) has previously been determined by observing the changes in both the ground and the excited state of the **btp** ligand.²³ From the $\text{Tb}(\text{III})$ luminescent changes, the binding constants were determined as being: $\log \beta_{1:3} = 22.7$, $\log \beta_{1:2} = 14.5 \pm 0.1$, and $\log \beta_{1:1} = 7.0$. While we attempted to fit the data obtained from the titrations shown in Fig. 6 and 7, then these gave not very reliable fits.



dually complex the Tb(III) ion. This was evidenced from the evolution of Tb(III)-centred emission in the fluorescence spectra at long wavelengths. However, Tb(III)-based emission from $^5D_4 \rightarrow ^7F_J$ ($J = 6-0$) is not a singlet spin state emission, and hence, we monitored the Tb(III)-based emission *via* phosphorescence spectra that will be discussed further below.³³

The fluorescence emission properties of **P2** were also probed. Upon excitation of **P2** at 237 nm, analogous ligand-centred fluorescence emission to **P1** was observed, localised at 335 nm (see ESI†) and, as in the case of **P1**, addition of Tb(III) efficiently quenched the ligand fluorescence due to metal coordination to the **btP** ligand, ultimately being reduced to 87% of the original emission intensity upon the addition of 0.5 equivalents of Tb(III).

Lanthanide luminescence changes. As discussed in the previous section, we observed quenching of the fluorescence of the ligands upon the addition of Tb(III) which suggested successful sensitisation of the Tb(III) excited state (the so-called antenna effect)³¹ due to energy transfer from the **btP** to Tb(III).

The delayed Tb(III)-centred luminescence was recorded upon excitation at $\lambda = 237$ nm in parallel with the monitoring of fluorescence emission from the polymer (using the same sample). The spectra and binding isotherms from the titrations can be seen in Fig. 6 for **P1** and in Fig. 7 for **P2**, respectively.

As can be seen in Fig. 6, titrating **P1** with Tb(CF₃SO₃)₃ gives rise to Tb(III) luminescence that is progressively enhanced with increasing equivalents of Tb(III). A gradual enhancement was observed in this luminescence in going from 0 \rightarrow 0.3 equivalents of Tb(III), after which a more rapid increase was observed up to approximately 0.5 equivalents. The characteristic Tb(III)-centred emission bands were observed at $\lambda = 490, 545, 585, 622, 647, 667,$ and 675 nm, corresponding to radiative deactivation from the $^5D_4 \rightarrow ^7F_J$ states. Subsequent additions of Tb(III), from 0.5 to 3.0 equivalents, resulted in no noticeable changes in the luminescence, indicating the formation of a stable Tb(III) complex with a 1:2 (M:L) stoichiometry. This species is also the most emissive species in solution as, upon further addition of Tb(III), no noticeable changes in the emis-

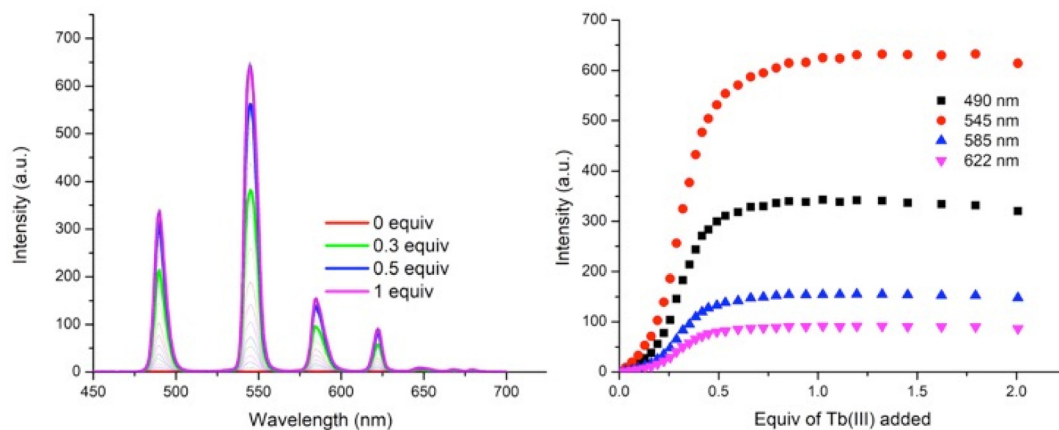


Fig. 6 The overall changes in the (left) Tb(III)-centred phosphorescence spectra ($\lambda_{\text{exc}} = 237$ nm) and (right) binding isotherms at $\lambda = 490, 545, 585$ and 622 nm upon titrating **P1** (1×10^{-5} M) against Tb(CF₃SO₃)₃ (0 \rightarrow 3 equiv.) in CH₃OH at RT. The equivalents added are in respect to the ligand concentration.

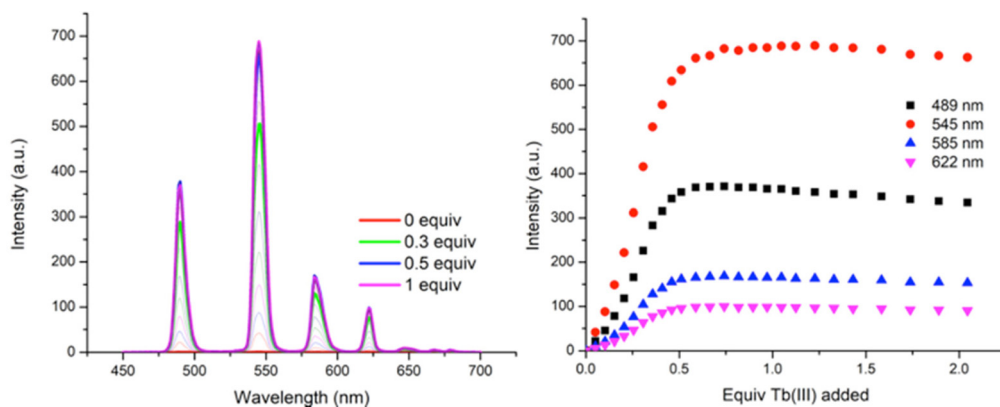


Fig. 7 The overall changes in the (left) Tb(III)-centred phosphorescence spectra and (right) binding isotherms at $\lambda = 490, 545, 585, 622, 647, 667,$ and 656 nm upon titrating **P2** (1×10^{-5} M) against Tb(CF₃SO₃)₃ (0 \rightarrow 3 equiv.) in CH₃OH at RT.



sion intensity were observed. However, **btp** ligands are known to give rise to complexes with 1 : 3 (M : L) stoichiometries and analysis of the titration isotherm in Fig. 6 shows that at that point, the emission is *ca.* 60% switched on, being fully switched on at the 1 : 2 stoichiometry, with no changes in the emission intensity at higher stoichiometries. Analysis of the overall changes show that the initially slow onset of the emission can be explained by the presence of Tb(III) species whose coordination spheres are made up primarily of bound solvent molecules which can deactivate the excited state through their O–H oscillations. This phenomenon is possibly more pronounced for polymer **P1** –with its lower loading of **btp** ligands – as it is possible that, in the absence of **btp** moieties close to the metal ion, coordination to the Tb(III) ion could occur *via* other coordination moieties competing with coordinating solvent molecules, such as the carbonyl groups contained within the **p(E-alt-MA)** polymer itself. Therefore, the speciation in solution is necessarily complex, and random, with coordination to the metal ions during the titrations arising from a potential combination of **btp** units, polymer backbone and solvent molecules. However, it is important to note that at higher Tb(III) loadings the emission is not being appreciably enhanced or quenched. This feature means that cannot conclusively determine if additional ions are binding to the polymer backbone alone as such species are, in all likelihood, non-emissive as these sites do not possess an antenna that can effectively populate the Tb(III) excited state.

This effect of higher loading of **btp** ligands within the polymer does indeed seem to be important in affecting the emission properties, as upon measuring the delayed Tb(III)-centred luminescence arising from **P2** upon titrating with Tb(CF₃SO₃)₃, the aforementioned ‘slow onset’ of the Tb(III) emission was absent. The overall changes in the Tb(III) emission of **P2** upon excitation at 237 nm is shown in Fig. 7. A gradual enhancement in the Tb(III) luminescence was observed up to the addition of 0.5 equivalents of the metal, with characteristic Tb(III)-centred emission transitions appearing at $\lambda = 490, 545, 585, 622, 647, 667,$ and 656 nm. Subsequent additions of Tb(III) did not result in any change in the luminescence intensity,

which indicates the formation of stable emissive species in solution.

While the concentration of compound **1** was the same within these two samples (1×10^{-5} M), and hence, for each titration, the higher number of grafted **btp** ligands at the backbone of the polymer **P(E-alt-MA)** in **P2** would increase the probability of forming cross-linked moieties (*e.g.* more of bridged ML₂ points within the polymer). Hence, the likelihood of the existence of great numbers of crosslinking structures exists within **P2** than **P1**. This indicates that subtle changes to the loading levels of **btp** units within the **p(E-alt-MA)** polymers can have profound effects on the subsequent self-assembly of the polymer with metal ions. With this in mind, and to gain further insights into the M : L stoichiometries of the polymer assemblies, we carried out studies on mixtures of Tb(III) and ligand **1**. The results (see ESI[†]) indeed showed that the 2 : 1 complex was the only observed signal in the HRMS, with the calculated and experimental isotopic distribution patterns matching a molecular species of the formula [Tb(1)₂](CF₃SO₃)₂⁺. While this does not exclude the formation of the 1 : 3 stoichiometry, as discussed above, it does seem to indicate that in the case of **1** the 1 : 2 stoichiometry is the most likely and/or the most stable structure to form upon self-assembly with Tb(III), supporting our observations from the ground and excited state measurements for **P1** and **P2**. Although traditionally the most emissive species possess the 1 : 3 stoichiometry, we have nevertheless observed efficient Tb(III)-based luminescence from both polymers upon titrating Tb(III). In addition, this 1 : 2 M : L stoichiometry is more than enough to structurally modify the polymer materials with the lanthanide ions acting to crosslink neighbouring polymer chains while the coordination sphere about the Tb(III) ions being completed by solvent molecules and/or coordination by carbonyl moieties on the polymer backbones. Accordingly, the presence of multiple different, competing coordinating species means that such crosslinking is likely to be random, but nevertheless would be expected to modulate the mechanical properties of such systems. Such studies are currently on going in our laboratory.

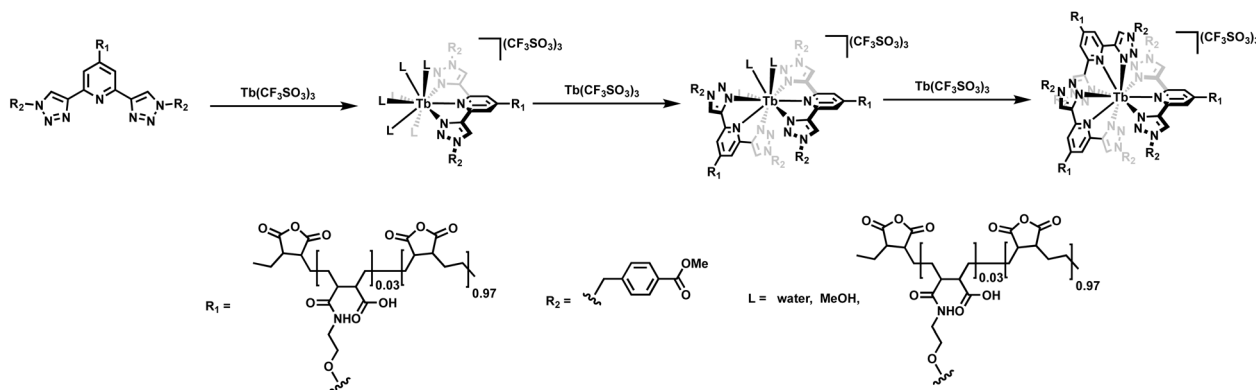


Fig. 8 The stepwise formation of the 1 : 1, 1 : 2 and 1 : 3 (M : L) stoichiometries possible with the **btp** ligands alone within the polymer.



Conclusions

In this study, we have developed two new CH₃OH and water-soluble polymers **P1** and **P2**, generated by modifying the polymer backbone of **P(E-*alt*-MA)** with the **btp** ligand **1**. By using UV-visible absorption and emission spectroscopies, we showed that these polymers could complex Tb(III) and form highly luminescent, cross-linked polymer structures. Analysis of the spectroscopic changes clearly demonstrate the formation of stable complexes exhibiting 1:2 (M:L) stoichiometries between the **btp**-based polymers (**P1** and **P2**) and Tb(III). However, given the high coordination requirements of the lanthanides, other stoichiometries can also occur. Furthermore, it cannot be ruled out that the backbone of the **P(E-*alt*-MA)** polymer itself takes part in the coordination of the ions. However, as no changes in the Tb(III)-centered emission were seen at high ion loadings, if such coordination is occurring, it does not affect the photophysical properties of the polymers. With the view of depicting the coordination environment around the **btp** units alone within the polymer, and with the view of showing the three dimensional nature of the cross-linking, we have drawn the three different M:L coordination environments in Fig. 8 in a schematic manner. It is important to note that we show these in the stepwise manner (1:1, 1:2 and 1:3 M:L). However, upon higher loading of the Tb(III) ions within the polymer, the reverse effect can also occur where the ligands in the 1:3 (which is commonly the most stable stoichiometry, with the ligands fulfilling the 9-coordination environment of the ion) are stripped off due to increasing Tb(III) concentrations. This we have seen in many of our lanthanide titrations in the past. This normally leads to quenching in the lanthanide luminescence if the displaced ligands are exchanged for O–H oscillators as we discussed above. However, the fact that the emission is not quenched above 0.5 equivalents, would indicate that the lanthanide centre is shielded from such coordination, possibly by the polymer backbone. We are in the process of developing other examples of lanthanide-based polymers and supramolecular polymers that utilise the **btp** motif.

Experimental

Materials and methods

All chemicals and solvents were obtained commercially and used without further purification. All NMR spectra were recorded using a Bruker Avance III 600 NMR spectrometer operating at 400 MHz for ¹H NMR and 101 MHz for ¹³C NMR. Chemical shifts (δ) were referenced relative to the internal solvent signals. The synthesis and characterisation of **1** has been previously reported and is only given here for a reference.²³

Synthesis of **1**

Dimethyl-4,4'-(((4-(2-aminoethoxy)pyridine-2,6-diyl)bis(1H-1,2,3-triazole-4,1-diyl))bis(methylene))dibenzoate (1**)**. Ligand

1 was obtained as a brown solid in 80%. The product decomposes over 182 °C. HRMS (m/z) (ESI+): calculated for C₂₉H₂₉N₈O₅H⁺ m/z = 569.2261 [M + H]⁺. Found m/z = 569.2266; ¹H NMR (400 MHz, DMSO): δ = 8.70 (s, 2H, triazol H), 7.98 (d, J = 8.2 Hz, 4H, Ar H–COOMe), 7.54 (s, 2H, pyridine H), 7.46 (d, J = 8.2 Hz, 4H, Ar H–CH₂), 5.81 (s, 4H, CH₂), 4.31 (t, J = 4.3 Hz, 2H, O–CH₂), 3.84 (s, 6H, OCH₃), 3.15 (q, J = 4.3 Hz, 2H, N–CH₂), ¹³C NMR (150 MHz, DMSO): δ = 165.8, 151.5, 147.2, 141.1, 129.7, 129.4, 128.5, 128.1, 124.1, 104.9, 64.7, 52.6, 52.2, 38.2. IR ν_{\max} (cm⁻¹): 3112, 3088, 3086, 2955, 2478, 2203, 2091, 1933, 1865, 1796, 1714, 1685, 1610, 1281, 1174, 1041, 801.

Synthesis and characterisation of P1/P2. Poly(ethylene-*alt*-maleic anhydride) (0.25 g, 0.006 mmol) was dissolved in anhydrous DMF (3 mL) under Ar and to this mixture, **1** (**P1**, 30 mg, 3 mol%; **P2**, 60 mg, 6 mol%) was added dropwise dissolved in DMF (2 mL). The solution was stirred at RT for 1 hour. Addition of 0.5 M HCl dropwise to this solution resulted in a white precipitate being formed that was filtered off and dried giving (277 mg, 98%); ¹H NMR (600 MHz, DMSO): δ = 12.36 (s, OH), 8.67 (s, 2H, triazole H), 7.99 (m, 4H, Ar H–COOMe), 7.50 (s, 2H, pyr H), 7.46 (m, 4H, Ar H–CH₂), 5.79 (s, 4H, CH₂), 3.84 (s, 6H, OCH₃), 3.05 (s, 69H, Hc and Hd), 0.85–1.96 (br m, polymer backbone).

Conflicts of interest

There are no conflicts to declare.

Acknowledgements

We would like to thank Science Foundation Ireland (SFI) (SFI PI Award 13/IA/1865 to T. G.) and (the SFI funded) Solid-State Pharmaceutical Centre (SSPC, Research Centres Phase 2: 12/RC/2275_P2) for financial support. We would especially like to thank Drs Gary Hessman, John E. O'Brien and Manuel Ruether for the help with HRMS and NMR studies.

References

- (a) P. K. Hashim, J. Bergueiro, E. W. Meijer and T. Aida, *Prog. Polym. Sci.*, 2020, **105**, 101250; (b) G. J. Scerri, M. Caruana, N. Agius, G. Agius, T. J. Farrugia, J. C. Spiteri, A. D. Johnson and D. C. Magri, *Molecules*, 2022, **27**, 5939; (c) T. Gorai, J. I. Lovitt, D. Umadevi, G. McManus and T. Gunnlaugsson, *Chem. Sci.*, 2022, **13**, 7805; (d) Y. Li, D. J. Young and X. J. Loh, *Mater. Chem. Front.*, 2019, **3**, 1489.
- (a) A. J. Savyasachi, O. Kotova, S. Shanmugaraju, S. J. Bradberry, G. M. Ó. Máille and T. Gunnlaugsson, *Chem*, 2017, **3**, 764; (b) M. Coste, E. Suárez-Picado and S. Ulrich, *Chem. Sci.*, 2022, **13**, 909; (c) G. Olivo, G. Capocasa, D. Del Giudice, O. Lanzalunga and S. Di Stefano, *Chem. Soc. Rev.*, 2021, **50**, 7681; (d) E. R. Draper



- and D. J. Adams, *Chem*, 2017, **3**, 390; (e) E. R. Draper and D. J. Adams, *Langmuir*, 2019, **35**, 6506.
- 3 (a) J.-F. Lutz, J.-M. Lehn, E. W. Meijer and K. Matyjaszewski, *Nat. Rev. Mater.*, 2016, **1**, 16024; (b) Y. Liu, Z. Wang and X. Zhang, *Chem. Soc. Rev.*, 2012, **41**, 5922; (c) A. B. Aletti, S. Blasco, S. J. Aramballi, P. E. Kruger and T. Gunnlaugsson, *Chem*, 2019, **5**, 2617; (d) T. Gunnlaugsson, *Nat. Chem.*, 2016, **8**, 6; (e) Y. T. Shen, C. H. Li, K. C. Chang, S. Y. Chin, H. A. Lin, Y. M. Liu, C. Y. Hung, H. F. Hsu and S. S. Sun, *Langmuir*, 2009, **25**, 8714; (f) A. D. Lynes, C. S. Hawes, K. Byrne, W. Schmitt and T. Gunnlaugsson, *Dalton Trans.*, 2018, **47**, 5259; (g) J. Kopeček, *Biomaterials*, 2007, **56**, 1078–1109.
- 4 (a) D. Zhao, J. Yang, Y. Wang and H. Li, *Dyes Pigm.*, 2022, **197**, 109864; (b) O. Kotova, S. J. Bradberry, A. J. Savyasachi and T. Gunnlaugsson, *Dalton Trans.*, 2018, **47**, 16377; (c) I. N. Hegarty, H. L. Dalton, A. D. Lynes, B. Haffner, M. E. Möbius, C. S. Hawes and T. Gunnlaugsson, *Dalton Trans.*, 2020, **49**, 7364; (d) S. Wei, Z. Li, W. Lu, H. Liu, J. Zhang, T. Chen and B. Z. Tang, *Angew. Chem., Int. Ed.*, 2021, **60**, 8608; (e) G. C. Le Goff, R. L. Srinivas, W. A. Hill and P. S. Doyle, *Eur. Polym. J.*, 2015, **72**, 386.
- 5 (a) S. Afzala and U. Maitra, *Helv. Chim. Acta*, 2022, **105**, e202100194; (b) T. Gorai and U. Maitra, *Angew. Chem., Int. Ed.*, 2017, **56**, 10730; (c) R. Laishram and U. Maitra, *Chem. Commun.*, 2022, **58**, 3162; (d) J. C. Yuan, X. L. Fang, L. X. Zhang, G. N. Hong, Y. J. Lin, Q. F. Zheng, Y. Z. Xu, Y. H. Ruan, W. G. Weng, H. P. Xia and G. H. J. Chen, *Mater. Chem.*, 2012, **22**, 11515; (e) B. Yang, H. Zhang, H. Peng, Y. Xu, B. Wu, W. Weng and L. Li, *Polym. Chem.*, 2014, **5**, 1945.
- 6 (a) S. J. Bradberry, A. J. Savyasachi, R. D. Peacock and T. Gunnlaugsson, *Faraday Discuss.*, 2015, **185**, 413; (b) S. J. Bradberry, G. Dee, O. Kotova, C. P. McCoy and T. Gunnlaugsson, *Chem. Commun.*, 2019, **55**, 1754.
- 7 (a) R. Daly, O. Kotova, M. Boese, T. Gunnlaugsson and J. J. Boland, *ACS Nano*, 2013, **7**, 4838; (b) O. Kotova, R. Daly, C. L. M. dos Santos, P. E. Kruger, J. J. Boland and T. Gunnlaugsson, *Inorg. Chem.*, 2015, **54**, 7735; (c) M. Martínez-Calvo, O. Kotova, M. E. Möbius, A. P. Bell, T. McCabe, J. J. Boland and T. Gunnlaugsson, *J. Am. Chem. Soc.*, 2015, **137**, 1983.
- 8 (a) E. M. Surender, S. J. Bradberry, S. A. Bright, C. P. McCoy, D. C. Williams and T. Gunnlaugsson, *J. Am. Chem. Soc.*, 2017, **139**, 381; (b) C. P. McCoy, F. Stomeo, S. E. Plush and T. Gunnlaugsson, *Chem. Mater.*, 2006, **18**, 4336.
- 9 O. Kotova, C. O'Reilly, S. T. Barwich, L. E. Mackenzie, A. D. Lynes, A. J. Savyasachi, M. Ruether, R. Pal, M. E. Möbius and T. Gunnlaugsson, *Chem*, 2022, **8**, 1395.
- 10 (a) D. E. Barry, D. F. Caffrey and T. Gunnlaugsson, *Chem. Soc. Rev.*, 2016, **45**, 3244; (b) T. Gunnlaugsson and F. Stomeo, *Org. Biomol. Chem.*, 2007, **5**, 1999; (c) T. Gunnlaugsson and J. P. Leonard, *Chem. Commun.*, 2005, **25**, 3114.
- 11 H. Xu, Q. Sun, Z. An, Y. Wei and X. Liu, *Coord. Chem. Rev.*, 2015, **293–294**, 228.
- 12 Monographs in Supramolecular Chemistry No. 33, in *Supramolecular Chemistry in Biomedical Imaging*, ed. S. Faulkner, T. Gunnlaugsson and G. M. Ó. Máille, The Royal Society of Chemistry, 2022.
- 13 (a) A. B. Aletti, D. M. Gillen and T. Gunnlaugsson, *Coord. Chem. Rev.*, 2018, **354**, 98; (b) D. Parker, J. D. Fradgley and K.-L. Wong, *Chem. Soc. Rev.*, 2021, **50**, 8193; (c) S. E. Bodman and S. J. Butler, *Chem. Sci.*, 2021, **12**, 2716; (d) E. Mathieu, A. Sipos, E. Demeyere, D. Phipps, D. Sakaveli and K. E. Borbas, *Chem. Commun.*, 2018, **54**, 10021; (e) T. Gorai, W. Schmitt and T. Gunnlaugsson, *Dalton Trans.*, 2021, **50**, 770.
- 14 (a) L. E. MacKenzie and R. Pal, *Nat. Rev. Chem.*, 2021, **5**, 109; (b) J. Andres, R. D. Hersch, J.-E. Moser and A.-S. Chauvin, *Adv. Funct. Mater.*, 2014, **24**, 5029.
- 15 (a) E. P. McCarney, J. P. Byrne, B. Twamley, M. Martínez-Calvo, G. Ryan, M. E. Mobius and T. Gunnlaugsson, *Chem. Commun.*, 2015, **51**, 14123; (b) I. N. Hegarty, H. L. Dalton, A. D. Lynes, B. Haffner, M. E. Möbius, C. S. Hawes and T. Gunnlaugsson, *Dalton Trans.*, 2020, **49**, 7364.
- 16 (a) A. F. Henwood, I. N. Hegarty, E. P. McCarney, J. I. Lovitt, S. Donohoe and T. Gunnlaugsson, *Coord. Chem. Rev.*, 2021, **449**, 214206; (b) J. P. Byrne, J. A. Kitchen and T. Gunnlaugsson, *Chem. Soc. Rev.*, 2014, **43**, 5302; (c) J. P. Byrne, J. A. Kitchen, O. Kotova, V. Leigh, A. P. Bell, J. J. Boland, M. Albrecht and T. Gunnlaugsson, *Dalton Trans.*, 2014, **43**, 196; (d) D. Preston and P. E. Kruger, *Chem. – Eur. J.*, 2019, **25**, 178; (e) Y. Li, J. C. Huffman and A. H. Flood, *Chem. Commun.*, 2007, **26**, 2692.
- 17 (a) Q. V. C. van Hilst, N. R. Largesse, D. Preston and J. D. Crowley, *Dalton Trans.*, 2018, **47**, 997; (b) H. Hofmeier and U. S. Schubert, *Chem. Soc. Rev.*, 2004, **33**, 373; (c) J. D. Crowley and P. H. Bandeen, *Dalton Trans.*, 2010, **39**, 612; (d) Q. V. C. van Hilst, R. A. S. Vasdev, D. Preston, J. A. Findlay, S. Ø. Scottwell, G. I. Giles, H. J. L. Brooks and J. D. Crowley, *Asian J. Org. Chem.*, 2019, **8**, 496; (e) J. E. M. Lewis, F. Modicom and S. M. Goldup, *J. Am. Chem. Soc.*, 2018, **140**, 4787; (f) M. Cirulli, A. Kaur, J. E. M. Lewis, Z. Zhang, J. A. Kitchen, S. M. Goldup and M. M. Roessler, *J. Am. Chem. Soc.*, 2019, **141**, 879; (g) Y. Li, M. Pink, J. A. Karty and A. H. Flood, *J. Am. Chem. Soc.*, 2008, **130**, 17293; (h) E. M. Zahran, Y. Hua, S. Lee, A. H. Flood and L. G. Bachas, *Anal. Chem.*, 2011, **83**, 3455; (i) D. Preston and P. E. Kruger, *Chem. – Eur. J.*, 2019, **25**, 1781; (j) D. A. W. Ross, D. Preston and J. D. Crowley, *Molecules*, 2017, **22**, 1762; (k) J. D. Crowley, P. H. Bandeen and L. R. Hanton, *Polyhedron*, 2010, **29**, 70.
- 18 C. O'Reilly, S. Blasco, B. Parekh, H. Collins, G. Cooke, T. Gunnlaugsson and J. P. Byrne, *RSC Adv.*, 2021, **11**, 16318.
- 19 J. P. Byrne, M. Martínez-Calvo, R. D. Peacock and T. Gunnlaugsson, *Chem. – Eur. J.*, 2016, **22**, 486.
- 20 J. P. Byrne, S. Blasco, A. B. Aletti, G. Hessman and T. Gunnlaugsson, *Angew. Chem., Int. Ed.*, 2016, **55**, 8938.
- 21 E. P. McCarney, J. I. Lovitt and T. Gunnlaugsson, *Chem. – Eur. J.*, 2021, **27**, 12052.



- 22 S. J. Bradberry, J. P. Byrne, C. P. McCoy and T. Gunnlaugsson, *Chem. Commun.*, 2015, **51**, 16565.
- 23 I. N. Hegarty, S. J. Bradberry, J. I. Lovitt, J. M. Delente, N. Fox, R. Daly and T. Gunnlaugsson, *Mater. Chem. Front.*, 2023, DOI: [10.1039/D2QM00998F](https://doi.org/10.1039/D2QM00998F), QM-RES-09-2022-000998 (at revision stage).
- 24 G. H. Hu and J. T. Lindt, *Polym. Bull.*, 1992, **29**, 357.
- 25 (a) D. E. Bergbreiter and Y. S. Liu, *Tetrahedron Lett.*, 1997, **38**, 3703; (b) C. Ladaviere, T. Delair, A. Domard, C. Pichot and B. Mandrand, *J. Appl. Polym. Sci.*, 1999, **71**, 927.
- 26 O. Stoilova, M. Ignatova, N. Manolova, T. Godjevargova, D. G. Mita and I. Rashkov, *Eur. Polym. J.*, 2010, 46.
- 27 Y. S. Choe, M. H. Yi, J. H. Kim, G. S. Ryu, Y. Y. Noh, Y. H. Kim and K. S. Jang, *Org. Electron.*, 2016, **36**, 171.
- 28 G. Panzarasa, A. Osypova, G. Consolati, F. Quasso, G. Soliveri, J. Ribera and F. Schwarze, *Nanomaterials*, 2018, **8**, 54.
- 29 C. Ladavière, T. Delair, A. Domard, C. Pichot and B. Mandrand, *J. Appl. Polym. Sci.*, 1999, **72**, 1565.
- 30 (a) E. P. McCahey, C. S. Hawes, J. A. Kitchen, K. Byrne, W. Schmitt and T. Gunnlaugsson, *Inorg. Chem.*, 2018, **57**, 3920; (b) I. N. Hegarty, H. L. Dalton, A. D. Lynes, B. Haffner, M. E. Möbius, C. S. Hawes and T. Gunnlaugsson, *Dalton Trans.*, 2020, **49**, 7364.
- 31 J. P. Byrne, J. A. Kitchen, J. E. O'Brien, R. D. Peacock and T. Gunnlaugsson, *Inorg. Chem.*, 2015, **54**, 1426.
- 32 D. Parker and J. A. G. Williams, *J. Chem. Soc., Dalton Trans.*, 1996, 3613.
- 33 J. C. G. Bünzli, *Acc. Chem. Res.*, 2006, **39**, 53.

